

THE ROLE OF KOZAI CYCLES IN NEAR-EARTH BINARY ASTEROIDS

JULIA FANG¹ AND JEAN-LUC MARGOT^{1,2}

¹ Department of Physics and Astronomy, University of California, Los Angeles, CA 90095, USA

² Department of Earth and Space Sciences, University of California, Los Angeles, CA 90095, USA

Received 2011 November 13; accepted 2011 December 29; published 2012 February 6

ABSTRACT

We investigate the Kozai mechanism in the context of near-Earth binaries and the Sun. The Kozai effect can lead to changes in eccentricity and inclination of the binary orbit, but it can be weakened or completely suppressed by other sources of pericenter precession, such as the oblateness of the primary body. Through numerical integrations including primary oblateness and three bodies (the two binary components and the Sun), we show that Kozai cycles cannot occur for the closely separated near-Earth binaries in our sample. We demonstrate that this is due to pericenter precession around the oblate primary, even for very small oblateness values. Since the majority of observed near-Earth binaries are not well separated, we predict that Kozai cycles do not play an important role in the orbital evolution of most near-Earth binaries. For a hypothetical wide binary modeled after 1998 ST27, the separation is large at 16 primary radii and so the orbital effects of primary oblateness are lessened. For this wide binary, we illustrate the possible excursions in eccentricity and inclination due to Kozai cycles as well as depict stable orientations for the binary's orbital plane. Unstable orientations lead to collisions between binary components, and we suggest that the Kozai effect acting in wide binaries may be a route to the formation of near-Earth contact binaries.

Key words: minor planets, asteroids: general – minor planets, asteroids: individual (2002 CE26, 2004 DC, 2003 YT1, Didymos, 1991 VH)

1. INTRODUCTION

About 15% of near-Earth asteroids (NEAs) larger than approximately 200 m in diameter are in a binary configuration (Margot et al. 2002; Pravec et al. 2006). These NEA binaries have dynamical lifetimes on the order of a few million years (Bottke et al. 2002) and are subject to a variety of perturbations, including close scattering encounters with terrestrial planets, radiative effects (called BYORP) from the Sun, tidal torques, and the Kozai mechanism. Such perturbative effects may change the orbital energy and angular momentum of the system, which can influence the binary's orbital elements, including semimajor axis, eccentricity, and inclination. We briefly discuss each of these perturbations next; their relevance in explaining observed spin and orbital data of NEA binaries is discussed in Fang & Margot (2012b).

The effect and frequency of close planetary encounters are studied by Fang & Margot (2012a), who found that approaches (<10 Earth radii) with Earth can occur for most observed NEA binaries on 1–10 million-year timescales. The radiative BYORP effect, while not observationally verified to date, is only relevant for satellites with spin–orbit synchronization. This effect has been theoretically found to be capable of modifying an NEA binary's semimajor axis and eccentricity on fast ($\sim 10^5$ years) timescales (Čuk & Burns 2005; Čuk 2007; Goldreich & Sari 2009; Čuk & Nesvorný 2010; McMahon & Scheeres 2010a, 2010b; Steinberg & Sari 2011). Tidal evolution of NEA binaries has been previously studied (see Taylor & Margot 2011, and references therein) and can cause spin–orbital synchronization as well as modify eccentricity (i.e., Goldreich 1963; Goldreich & Sari 2009). The Kozai mechanism (Kozai 1962), in the context of NEA binaries, has not been fully studied and is the focus of this paper.

The Kozai mechanism is very relevant for many astrophysical triple systems; examples include its influence on

the stability for irregular Jovian satellites with high inclinations (e.g., Nesvorný et al. 2003), main belt and trans-Neptunian binaries (Perets & Naoz 2009), asteroids and comets due to Jupiter (e.g., Kozai 1962; Thomas & Morbidelli 1996), binary stars with distant companions (Harrington 1968; Mazeh & Shaham 1979; Kiseleva et al. 1998; Eggleton & Kiseleva-Eggleton 2001; Eggleton & Kiseleva-Eggleton 2006; Fabrycky & Tremaine 2007), extrasolar planets with outlying perturbers (Mazeh et al. 1997; Innanen et al. 1997; Holman et al. 1997; Tremaine & Zakamska 2004; Takeda & Rasio 2005; Fabrycky & Tremaine 2007; Katz et al. 2011; Lithwick & Naoz 2011; Naoz et al. 2011), and binary supermassive black holes (Blaes et al. 2002).

In this paper, we consider the Kozai mechanism in terms of the following triple system: an NEA binary, consisting of a massive primary and less massive secondary, and the Sun as an outer perturber (as in Perets & Naoz 2009). The Kozai mechanism is a *secular* effect, i.e., the effect occurs on timescales that exceed the orbital periods. Analytical computation of secular effects traditionally involve averaging quantities over a complete orbital cycle. Under the Kozai effect, the secondary's orbit with respect to the primary will undergo coupled changes in eccentricity and inclination. We define the inclination as the relative inclination between the binary's mutual orbit and the binary's heliocentric orbit. For a circular heliocentric orbit, the coupled oscillations in eccentricity e and inclination i will conserve the quantity $\sqrt{1-e^2} \cos i$ such that for satellites in prograde orbits ($0^\circ \leq i < 90^\circ$), peaks in eccentricity correspond to minima in inclination, and vice versa. Satellites in retrograde orbits ($90^\circ \leq i \leq 180^\circ$) will have eccentricity and inclination oscillate in the same direction. In the absence of other perturbations, an initially circular binary will undergo large Kozai cycles if a critical inclination i is met: $39.2^\circ < i < 140.8^\circ$. Initially eccentric binaries will undergo Kozai cycles over a wider inclination range. For an initially circular binary,

Table 1
Sample of Near-Earth Binaries

System	R_p (km)	M_p (kg)	R_s (km)	M_s (kg)	n (deg day ⁻¹)	a (km)	e	R_{Hill} (km)	n_{\odot} (deg day ⁻¹)	a_{\odot} (AU)	e_{\odot}
(276049) 2002 CE26 ^a	1.75	2.17×10^{13}	0.150	1.37×10^{10}	554.34	4.87	0.025	514	0.30	2.23	0.56
2004 DC ^b	0.17	3.57×10^{10}	0.030	1.96×10^8	372.93	0.75	0.30	44	0.47	1.63	0.40
(164121) 2003 YT1 ^c	0.55	1.89×10^{12}	0.105	1.32×10^{10}	226.73	3.93	0.18	113	0.84	1.11	0.29
(65803) Didymos ^d	0.40	5.24×10^{11}	0.075	3.45×10^9	724.38	1.18	0.04	109	0.47	1.64	0.38
(35107) 1991 VH ^e	0.60	1.40×10^{12}	0.240	8.93×10^{10}	265.07	3.26	0.06	105	0.81	1.14	0.14
Hypothetical wide binary	0.42	7.73×10^{11}	0.050	1.51×10^9	65.46	6.66	0.3	62	1.33	0.82	0.53

Notes. This table consists of a subset of well-characterized NEA binaries whose uncertainty region for the orbital plane orientation includes the Kozai-acting regime ($39.2 < i < 140.8$) for initially circular binaries. In addition, we list a hypothetical wide binary modeled after 1998 ST27, whose actual physical and orbital properties are not well known. For all entries, we list adopted values for primary radius R_p , primary mass M_p , secondary radius R_s , secondary mass M_s , binary mean motion n , binary semimajor axis a , binary eccentricity e , the Hill radius R_{Hill} (beyond which the binary's components would be primarily orbiting the Sun instead of each other), heliocentric mean motion n_{\odot} , heliocentric semimajor axis a_{\odot} , and heliocentric eccentricity e_{\odot} . Binary parameters and uncertainties can be found in Fang & Margot (2012b), and heliocentric parameters and uncertainties can be found in the JPL Small Body Database.

^a Shepard et al. (2006).

^b Taylor et al. (2008).

^c Nolan et al. (2004).

^d Benner et al. (2010).

^e Margot et al. (2008) and Pravec et al. (2006).

the maximum eccentricity e_{max} that can be induced by the Kozai mechanism is

$$e_{\text{max}} = \sqrt{1 - \frac{5}{3} \cos^2 i_{\text{init}}}, \quad (1)$$

where i_{init} is the initial inclination (i.e., Innanen et al. 1997). If $i_{\text{init}} \sim 90^\circ$, then the binary's eccentricity will grow to ~ 1 during a single Kozai oscillation. The approximate oscillation timescale or Kozai period P_K is on the order of (Kiseleva et al. 1998)

$$P_K = \frac{2P_{\odot}^2}{3\pi P} (1 - e_{\odot}^2)^{3/2} \frac{M_p + M_s + M_{\odot}}{M_{\odot}}, \quad (2)$$

where the binary's mutual orbit has period P , the primary's mass is M_p , the secondary's mass is M_s , the Sun's mass is M_{\odot} , the heliocentric orbital period is P_{\odot} , and the heliocentric eccentricity is e_{\odot} . The Kozai effect due to the Sun for binaries in the solar system is much more pronounced for NEAs than for main belt and trans-Neptunian objects because P_K varies as the square of the heliocentric orbital period P_{\odot} .

Among the population of well-characterized NEA systems compiled by Fang & Margot (2012b), we list in Table 1 only binary systems for which the uncertainty region in orbital plane orientation includes the Kozai regime ($39.2 < i < 140.8$) for initially circular binaries. This criterion rules out two triple systems, 2001 SN263 and 1994 CC, and two binary systems, 2000 DP107 and 1999 KW4, for which the Kozai effect will not operate (Fang & Margot 2012b). We also include a hypothetical wide binary modeled after 1998 ST27, which is the widest NEA binary known so far but unfortunately has binary orbital and physical parameters that are not well determined. For the hypothetical binary's heliocentric orbital elements listed in Table 1, we use 1998 ST27's actual heliocentric orbital elements, which are well known.

The goal of this study is to investigate the relevance and effect of Kozai cycles in the presence of other modulating perturbations. The outline of this paper is as follows. In Section 2, we describe other perturbations—the primary's oblateness, additional satellites, and tidal effects—that may damp Kozai cycles and we find that primary oblateness is dominant. In Section 3, we perform numerical investigations of the Kozai effect modulated by primary oblateness for all binaries in our sample, and

determine their excursions in eccentricity and inclination. In Section 4, we discuss the implications of this work, including the role of Kozai cycles in the evolution of most NEA binaries, constraints on orbital plane orientations, how Kozai-induced instabilities end in collisions, and the formation of contact binaries. We briefly summarize this study in Section 5.

2. PERTURBATIONS THAT AFFECT KOZAI CYCLES

Here, we consider effects that can weaken or completely suppress Kozai cycles. The Kozai effect causes oscillations in eccentricity and inclination, and systems in Kozai resonance can exhibit libration of the argument of pericenter.

Given that this effect is caused by the interaction between the shape of the binary's mutual orbit and weak solar tides, Kozai cycles can be easily suppressed by other weak perturbations that contribute to apsidal (pericenter) precession in the binary. If the argument of pericenter precesses too fast, libration of the argument of pericenter is no longer possible, which inhibits the Kozai process.

In the following subsections, we consider contributions to pericenter precession from three effects: the primary's non-spherical shape leading to a non-uniform gravitational field with a quadrupole moment (J_2) representing the degree of oblateness, the presence of additional, undetected satellites, and tidal bulges due to both the primary and the secondary. These effects can potentially weaken or suppress Kozai cycles, and we seek to determine their relative strengths.

2.1. Primary Oblateness (J_2)

We consider the contribution to pericenter precession caused by primary oblateness. Many NEAs have non-spherical shapes, and the level of oblateness can be described by a coefficient, J_2 , as (Murray & Dermott 1999)

$$J_2 = \frac{C - (A + B)/2}{M_p R_p^2} \approx \frac{C - A}{M_p R_p^2}, \quad (3)$$

where A , B , and C are the primary's moments of inertia. M_p is the primary's mass and R_p is the primary's equatorial radius. The approximation is valid when $A \approx B$.

Table 2
Pericenter Precession Rates

System	Pericenter Precession (deg day ⁻¹)		
	$\dot{\omega}_{J_2}$	$\dot{\omega}_{\text{sat}}$	$\dot{\omega}_{\text{tides}}$
2002 CE26	0.22–22	<3.5e-6	5.0e-7–3.1e-5
2004 DC	0.069–6.9	<5.6e-3	5.7e-8–8.2e-5
2003 YT1	0.014–1.4	<2.8e-4	8.6e-9–1.0e-6
Didymos	0.25–25	<2.2e-4	1.3e-6–3.0e-4
1991 VH	0.027–2.7	<1.9e-4	3.3e-7–8.3e-6
HWB ^a	0.00094–0.094	<1.4e-4	1.5e-11–6.7e-9

Notes. Rates for the argument of pericenter ω are calculated for each binary and for three main sources of pericenter precession: primary's J_2 , an additional satellite, and tidal bulges raised on the primary and secondary. A range of rates is given for the effects of oblateness, corresponding to J_2 values from 0.001 to 0.1. A range of rates is given for the effects of tides, corresponding to two different tidal Love number models (Goldreich & Sari 2009; Jacobson & Scheeres 2011). Precession due to an additional satellite assumes a size of 30 m. ^a HWB = hypothetical wide binary modeled after 1998 ST27.

The J_2 coefficient is an indirectly observable quantity that can be detected by its non-Keplerian effects induced on orbiting satellites. Such oblateness-induced precession on the orbits of satellites can be examined by the rate of change in the argument of pericenter ω (Vallado 2001):

$$\frac{d\omega}{dt_{J_2}} = \frac{3}{2} \frac{n J_2}{(1 - e^2)^2} \left(\frac{R_p}{a} \right)^2 \left(\frac{5}{2} \cos^2 I - \frac{1}{2} \right), \quad (4)$$

where n is the binary's mean motion, e is the eccentricity, R_p is the primary's radius, a is the semimajor axis, and I is the binary's orbital inclination relative to the primary's equator. The J_2 effect is more relevant for asteroid binaries than their trans-Neptunian counterparts because asteroid binaries tend to be separated by several primary radii and trans-Neptunian binaries are typically much wider. The orbits of close-in satellites will be more perturbed by an oblate primary than the orbits of distant satellites, since Equation (4) shows that precession due to J_2 varies inversely as distance squared.

The primary's J_2 value for most NEA binaries is unknown; we calculate a range of values for apsidal precession due to J_2 coefficients ranging from 0.001 to 0.1. A few well-characterized NEA systems have known shapes and J_2 values, including 1999 KW4 (Ostro et al. 2006) with a primary J_2 of ~ 0.06 and 1994 CC (Brozovic et al. 2011) with a primary J_2 of ~ 0.01 . In our calculations, we assume that the satellite is orbiting in the equatorial plane of the primary (support for this assumption comes from the generally accepted rotational fission formation model; Margot et al. 2002; Pravec et al. 2006; Walsh et al. 2008), and we use nominal values of their current separations and eccentricities. These numbers are presented in Table 2.

2.2. Additional Satellite

We examine if the presence of an additional satellite (presumably undetected) in the asteroid system can suppress Kozai oscillations by causing the known satellite's orbit to precess. It is known that the presence of larger, detectable satellites can easily suppress Kozai cycles, as shown through numerical simulations by Fang et al. (2011) for NEA triple systems 2001 SN263 and 1994 CC and as discussed by Ragozzine & Brown (2009) for trans-Neptunian triple Haumea. Here, we investigate if a small, unobserved satellite can also damp Kozai cycles.

Since most NEA binaries are discovered by planetary radar, we adopt a fairly common value of the spatial resolution in radar images (15 m) as the typical radius of the additional satellite in our study. This is adopted for convenience and does not represent the finest spatial resolution available nor the radar detectability threshold. If a small, undetectable satellite can damp Kozai cycles, then it may be responsible for the survival of NEA systems that would otherwise undergo high oscillations in eccentricity and inclination.

In the presence of an additional satellite, both satellites will undergo time-averaged, secular changes in their orbital elements. For a coplanar system, their argument of pericenter rates are (Mardling 2007)

$$\frac{d\omega_{s1}}{dt_{\text{sat}}} = \frac{3}{4} n_{s1} \left(\frac{M_{s2}}{M_p} \right) \left(\frac{a_{s1}}{a_{s2}} \right)^3 (1 - e_{s2}^2)^{3/2} \times \left[1 - \frac{5}{4} \left(\frac{a_{s1}}{a_{s2}} \right) \left(\frac{e_{s2}}{e_{s1}} \right) \frac{\cos(\omega_{s1} - \omega_{s2})}{1 - e_{s2}^2} \right] \quad (5)$$

$$\frac{d\omega_{s2}}{dt_{\text{sat}}} = \frac{3}{4} n_{s2} \left(\frac{M_{s1}}{M_p} \right) \left(\frac{a_{s1}}{a_{s2}} \right)^2 (1 - e_{s2}^2)^{-2} \times \left[1 - \frac{5}{4} \left(\frac{a_{s1}}{a_{s2}} \right) \left(\frac{e_{s1}}{e_{s2}} \right) \frac{(1 + 4e_{s2}^2)}{(1 - e_{s2}^2)} \cos(\omega_{s1} - \omega_{s2}) \right] \quad (6)$$

and these equations are given to fourth power in a_{s1}/a_{s2} and first order in e_{s1} . The subscripts $s1$ and $s2$ represent the inner and outer satellites, respectively, and the subscript p is for the primary. The equations also include the mean motion n , mass M , semimajor axis a , and eccentricity e . These equations are valid for $M_{s1} \ll M_p$, but there are no restrictions on M_{s2} .

We calculate the apsidal rates for each binary in Table 1, assuming a coplanar system. For each binary, the additional satellite is given a radius of 15 m and a typical rubble pile density of 2 g cm^{-3} with a circular orbit. For all binaries except the hypothetical wide binary modeled after 1998 ST27, we treat the observed satellite as the inner satellite and the additional, undetected satellite as the outer satellite with a semimajor axis of 15 primary radii (which is a typical separation for the outer satellite in an NEA triple, based on a sample of two known NEA triples). For the hypothetical wide binary, whose satellite is located at 6.66 km or 16 primary radii, we treat this satellite as the outer satellite and the undetected satellite as the inner satellite with a semimajor axis of 4 primary radii. In all cases, we use the observed satellite's current separation and eccentricity. Our calculated apsidal precession rates are shown in Table 2, which represent the pericenter precession due to a 30 m diameter satellite.

2.3. Tidal Bulges

For completeness we investigate tidal bulges raised on both the primary and secondary, although we anticipate their contribution to pericenter precession to be small. The argument of pericenter rate is (e.g., Sterne 1939; Fabrycky & Tremaine 2007; Batygin & Laughlin 2011)

$$\frac{d\omega}{dt_{\text{tides}}} = \frac{15}{16} n \left[\frac{8 + 12e^2 + e^4}{(1 - e^2)^5} \right] \times \left[k_p \left(\frac{R_p}{a} \right)^5 \left(\frac{M_s}{M_p} \right) + k_s \left(\frac{R_s}{a} \right)^5 \left(\frac{M_p}{M_s} \right) \right], \quad (7)$$

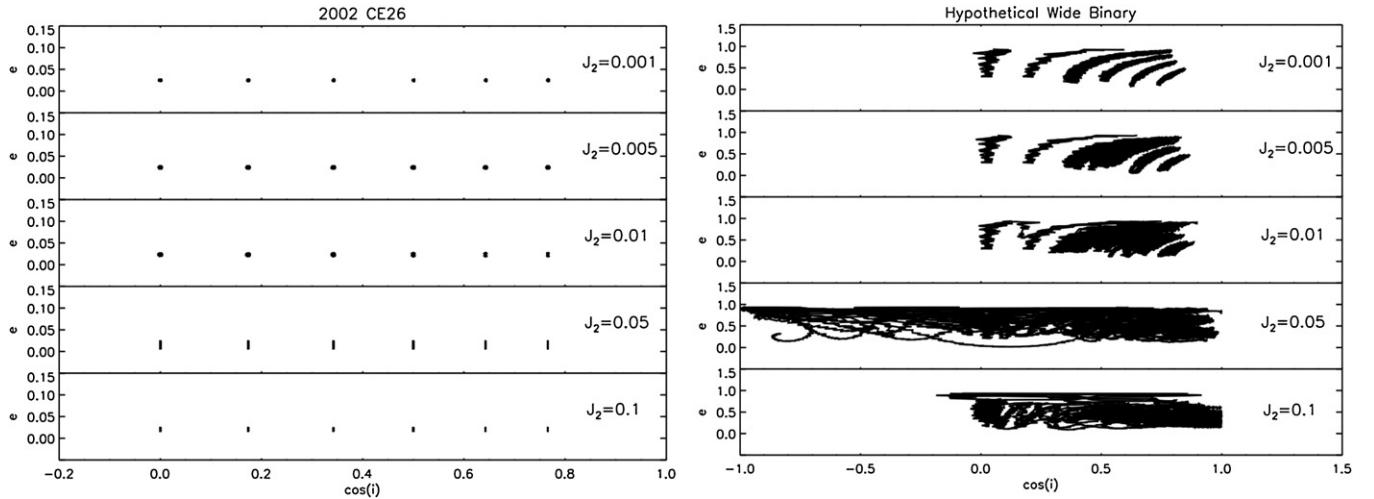


Figure 1. Results from all numerical simulations for 2002 CE26 (left) and for a hypothetical wide binary modeled after 1998 ST27 (right) are shown in these stacked plots with panels representing different J_2 values for the primary. The y-axis shows excursions in eccentricity e space and the x-axis illustrates the ranges of inclination i . In each panel, starting conditions include the observed separation and eccentricity as well as various values for the inclination and the argument of pericenter.

where the first term corresponds to the primary and the second term corresponds to the secondary. The equation also includes the mean motion n , eccentricity e , radius R , semimajor axis a , mass M , and tidal Love number k . Subscripts p and s stand for the primary and secondary, respectively.

The tidal Love number is a poorly known quantity for small rubble pile asteroids, and there are currently two different rubble pile models that describe the Love number’s dependence on size (or radius R). Goldreich & Sari (2009) give the relation $k_{\text{rubble}} \sim 10^{-5} (R/1 \text{ km})$, and Jacobson & Scheeres (2011) find that $k_{\text{rubble}} \sim 2.5 \times 10^{-5} (1 \text{ km}/R)$. Using both tidal Love number models and the binaries’ current separations and eccentricities, we calculate a range of possible apsidal precession rates due to tidal bulges for each NEA binary in Table 2.

Examination of the values in Table 2 indicates that even the smallest amount of primary oblateness (J_2 of 0.001) will dominate over all other perturbations; the contribution from each perturbation is quantified in Table 2 for all NEA binaries in our sample. Therefore, the numerical integrations described in the next section only include the effect of primary oblateness out of the three sources of pericenter precession considered here.

3. NUMERICAL INVESTIGATION

Through numerical simulations, we explore the excursion in a binary’s eccentricity and inclination due to three-body effects, such as Kozai cycles induced by the Sun, and we include perturbations due to primary oblateness. We use a Bulirsch–Stoer algorithm from *Mercury* (Chambers 1999) and our system is composed of three bodies: the Sun and primary and secondary components of the binary. For each binary in our investigation (Table 1), our integration time covers at least 10 Kozai oscillation periods with a time step that is 1/50th of the binary’s mutual orbital period. Initial conditions for each binary’s heliocentric semimajor axis and eccentricity as well as starting values for the masses, separations, and eccentricities of the binary components are taken from their known, observed values (Table 1).

For each binary in our sample, we perform an ensemble of simulations. In all simulations we assume that the binary’s mutual orbit is in the primary’s equatorial plane. We sample a range of J_2 values to approximate the primary’s non-spherical shape,

a range of inclinations between the binary’s mutual and heliocentric orbits, and a range of values for the binary’s argument of pericenter; none of these parameters are known for the binaries in our sample. Our choice of J_2 values includes 0.001, 0.005, 0.01, 0.05, and 0.1. Currently, the best-characterized NEA binary is 1999 KW4 (Ostro et al. 2006) with detailed shape and orbital information, and its primary has a J_2 value of ~ 0.06 . Another NEA system with known primary shape is 1994 CC (Brozovic et al. 2011), with a primary J_2 of ~ 0.01 . Our range of inclinations spans angles in the strongest Kozai-operating regime of 40° – 90° with 10° increments; these inclinations represent satellites in prograde orbits. Identical behavior, but mirrored across 90° , would be seen for inclinations greater than 90° representing retrograde orbits. We sample arguments of pericenter from 0° to 90° with 30° increments, as similar behavior is repeated for each 90° quadrant.

Our findings are as follows. Due to a non-zero J_2 , binaries 2002 CE26, Didymos, 2004 DC, and 1991 VH do not exhibit any expected Kozai behavior such as libration of the argument of pericenter or large excursions in eccentricity and inclination. Instead, the argument of pericenter circulates quickly and there are rapid, small-amplitude oscillations in eccentricity and inclination. Typical behavior for these binaries that do not exhibit expected Kozai cycles are illustrated in Figure 1 (left panel). This figure displays the results from all numerical simulations for 2002 CE26 by showing the eccentricity and inclination excursions. Moreover, if Kozai cycles are present, then in the absence of other perturbers we expect an initially circular binary to have an eccentricity increase (see Equation (1)) of ~ 0.15 for i_{init} of 40° , ~ 0.56 for i_{init} of 50° , ~ 0.76 for i_{init} of 60° , ~ 0.90 for i_{init} of 70° , ~ 0.97 for i_{init} of 80° , and 1 for i_{init} of 90° . Comparison between these values and Figure 1 (left panel) for 2002 CE26, an initially near-circular binary, provides additional evidence that the expected Kozai cycles are not present. For binary 2003 YT1, there are signs of Kozai cycles only with a J_2 as low as 0.001, where there are significant excursions in eccentricity and inclination; larger J_2 values suppress any Kozai oscillations.

Kozai cycles may induce collisional disruptions between the primary and secondary if the eccentricity grows large enough that the pericenter approaches 1 primary radius. This is more likely to occur at high inclinations (Equation (1)). For binaries

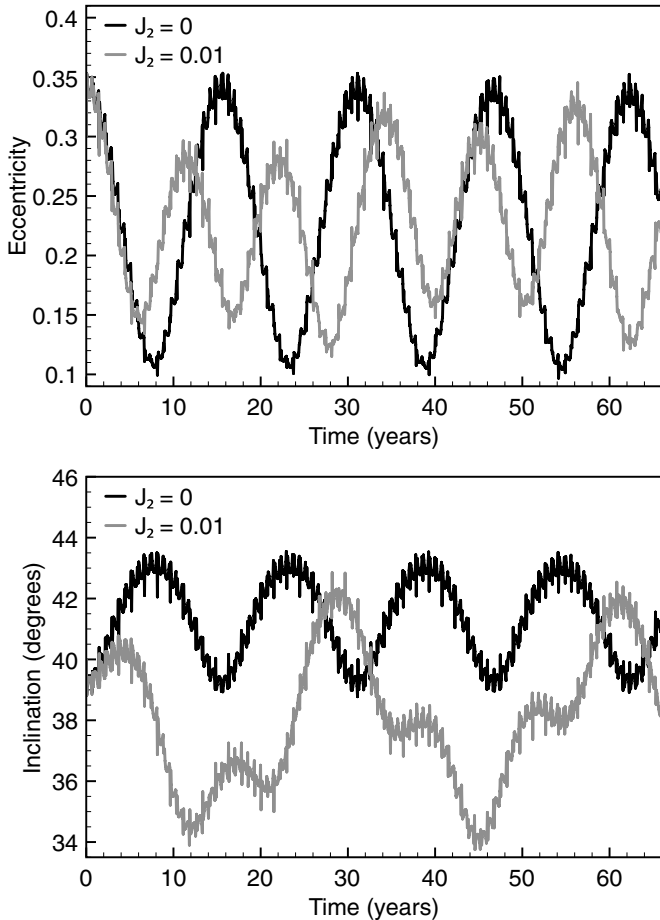


Figure 2. Comparison between pure Kozai cycles ($J_2 = 0$) and modulated Kozai cycles ($J_2 = 0.01$) for a hypothetical wide binary modeled after 1998 ST27. The starting conditions for this particular simulation are as follows: eccentricity is 0.3, inclination is 40° , and the argument of pericenter is 90° .

2002 CE26, 2004 DC, Didymos, 1991 VH, and 2003 YT1, collisional disruptions are expected at high inclinations yet not observed in any of our simulations for the entire explored range of J_2 values. None of the simulations for each of these binaries show any disruptions (i.e., collisions or ejections) during the nominal integration time, contrary to expected Kozai behavior that leads to high eccentricities within one cycle. The lack of disruptions in non-zero J_2 cases provides further confirmation that expected Kozai behavior is not present when we include the effects of primary oblateness.

For the hypothetical wide binary modeled after 1998 ST27, Kozai cycles are present with the complete range of J_2 values sampled here. In the case of high J_2 values, the system exhibits wide, overlapping excursions in eccentricity and inclination (Figure 1 (right panel)). These Kozai cycles are modulated by a non-zero J_2 ; Figure 2 illustrates a comparison of pure Kozai cycles versus Kozai cycles under the influence of J_2 . This hypothetical binary exhibits Kozai behavior as opposed to the other binaries in our sample because it is the most widely separated system with its satellite stationed at a relatively far separation of 16 primary radii. Therefore, solar perturbations are stronger than the effects induced by primary oblateness. For this hypothetical wide binary only, we continue integrating its ensemble of numerical simulations to 10^5 years to obtain more accurate disruption statistics. We find that Kozai-induced disruptions occur in $\sim 44\%$ of all cases examined here, with collisions and

not ejections as the only observed disruption outcomes. See Section 4 for discussion regarding such instabilities.

These numerical integrations suggest that the evolution of most observed NEA binaries are dominated by primary oblateness rather than the Kozai effect. This conclusion is also supported by an analytical comparison between the two effects. For all well-characterized binaries, Fang & Margot (2012b) calculated the critical semimajor axis separating the influence regions of primary oblateness and solar dynamics as (Nicholson et al. 2008)

$$a_{\text{crit}} = \left(2J_2 \frac{M_p}{M_\odot} R_p^2 a_\odot^3 \right)^{1/5}, \quad (8)$$

where J_2 represents the extent of primary oblateness, M_p is the primary's mass, M_\odot is the Sun's mass, R_p is the primary's radius, and a_\odot is the heliocentric semimajor axis. Fang & Margot (2012b) found that the range of allowable a_{crit} values corresponding to J_2 values ranging from 0.001 to 0.1 were greater than observed semimajor axes for all well-characterized NEA binaries; they are oblateness-dominated. We also calculate a_{crit} for the hypothetical wide binary modeled after 1998 ST27. For this hypothetical binary, a_{crit} ranges from 3.02 to 7.60 km and so could be larger or smaller than the adopted semimajor axis of 6.66 km. Therefore, this hypothetical binary could be in the oblateness-dominated or Kozai-dominated regime. This analysis shows general consistency with the results from numerical simulations; binaries predicted to be oblateness-dominated by Equation (8) do not show expected Kozai oscillations in numerical simulations, and the hypothetical wide binary predicted to be either oblateness- or solar-dominated does show strong signs of Kozai cycles modulated by J_2 . Accordingly, tightly bound binaries (those that exhibit no signs of the Kozai effect) are strongly affected by primary oblateness and loosely bound binaries (showing Kozai oscillations) are less perturbed by the far-away primary's oblateness.

4. DISCUSSION

In this section, we discuss each of the following in turn: the relevance of Kozai cycles for observed NEA binaries, orbit orientation constraints for wide binaries that can undergo Kozai oscillations, collisions as the only disruption outcome due to the Kozai effect for typical NEA binaries, and Kozai cycles as a possible route to the formation of contact binaries.

4.1. General Population of Observed NEA Binaries

We extrapolate from our simulation results to the observed NEA binary population. Numerical integrations in Section 3 demonstrated that four out of five well-characterized NEA binaries in our sample (Table 1) showed no signs of Kozai cycles and the exception, 2003 YT1, only showed evidence of Kozai cycles when the primary had a very minimal level of oblateness ($J_2 = 0.001$). All five of these well-characterized binaries have semimajor axes less than 8 primary radii. Only the hypothetical wide binary (at 16 primary radii) modeled after 1998 ST27 exhibited signs of Kozai cycles at a range of J_2 values from 0.001 to 0.1. The effects of primary oblateness are strongest for close-in binaries (pericenter precession due to J_2 increases as the semimajor axis squared; Equation (4)), where an oblate primary can cause the satellite's orbital plane to precess fast enough to thwart any Kozai oscillations.

If we consider all well-characterized NEA binaries as compiled by Fang & Margot (2012b), none of them have separations

greater than 8 primary radii. In fact, the semimajor axes of all of these well-characterized NEA binaries are within the range of semimajor axes of the binaries in our sample, which did not show Kozai cycles at a range of plausible J_2 values. If we consider this list of well-characterized NEA binaries to be representative of the observed population of NEA binaries, then typical NEA binaries do not appear to be affected by Kozai cycles in their orbital evolution. We point out a mild selection effect in that most well-characterized NEA binaries have made close enough approaches to Earth to be detected by radar, and this subset of the population may have fewer wide binaries than the general population. One could argue that we mostly observe binaries immune from Kozai effects because the Kozai-acting binaries have disrupted on short Kozai timescales (see following subsections on disruptions and contact binary formation). However, our simulations show that the requirements on primary oblateness and component separation are quite stringent, and we conclude that Kozai cycles are unlikely to be an important effect in most NEA binaries.

4.2. Constraints on Orbit Pole Orientations

Orbit pole orientations can be constrained for binaries that undergo Kozai cycles. In Section 3, we explored a hypothetical wide binary modeled after 1998 ST27 that exhibited signs of Kozai oscillations and disruptions, and in this subsection we illustrate this binary’s stable orbit pole orientations. Stable orbit poles are defined as initial orientations that do not end in a collision after 10^5 years of numerical integrations; these results are based on the ensemble of simulations performed in Section 3 as well as additional simulations to sample the full range of inclinations. The range of inclinations corresponding to stable binaries allows us to calculate the corresponding J2000 ecliptic coordinates (latitude β and longitude λ) of binary orbits for stable binaries. Since the hypothetical wide binary under consideration is modeled after 1998 ST27, we use 1998 ST27’s well-known heliocentric orbit poles (ecliptic longitude of the ascending node = $197^\circ.5842$ and ecliptic inclination = $21^\circ.05458$) for our calculations.

In Figure 3, we map out constraints on the orbit orientations for this hypothetical wide binary, showing results for three different J_2 values for the primary: 0, 0.005, and 0.05. Color-coded lines (for different J_2 values) separate the “Kozai stable” and “Kozai unstable” regions. Regions where at least half of simulations resulted in stable binaries are called “Kozai stable,” and regions where over half of simulations resulted in unstable binaries are called “Kozai unstable.” This orbit orientation map provides constraints on allowable orientations because binaries that will disrupt under the effect of Kozai are unlikely to be observed with orbit ecliptic coordinates in the unstable regions of Figure 3. Most Kozai-induced disruptions occurred within 100 years, shorter than evolutionary timescales due to tides, BYORP, and close planetary encounters. Accordingly, for this hypothetical wide binary we can predict that its orbit does not lie in the region bounded by the color-coded J_2 lines. This analysis is performed here for this hypothetical wide binary and can similarly be applied to other binaries that can be affected by Kozai perturbations. We note that a different binary (presumably with a different heliocentric orbital pole) would result in a different layout of stable and unstable zones (i.e., stability islands).

Figure 3 also shows how different J_2 values can affect the stability map, discussed here for the hypothetical wide binary. For discrete J_2 values of 0, 0.001, 0.005, 0.01, and 0.05, we find

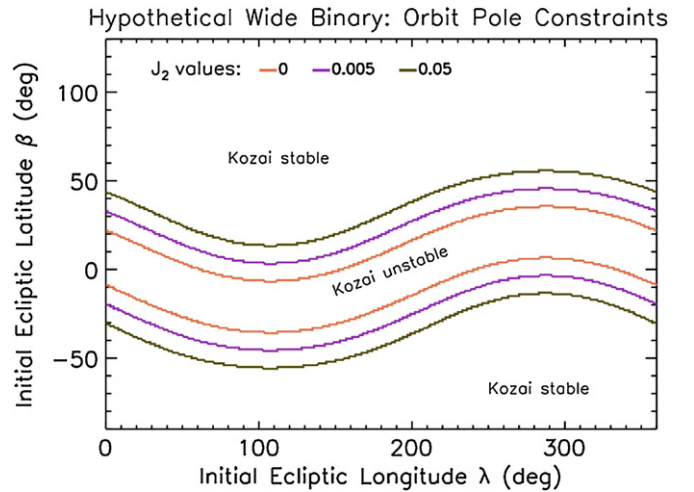


Figure 3. Stability map that shows constraints on initial orbit pole orientations for a hypothetical wide binary modeled after 1998 ST27. There are two regions: “Kozai stable” refers to regions where at least 50% of simulations resulted in stable binaries, and “Kozai unstable” refers to regions where more than 50% of simulations resulted in unstable binaries. Intermediate lines of varying colors (representing different J_2 values) separate “Kozai stable” and “Kozai unstable” regions. Stable orbit orientations cover roughly $\sim 75\%$, $\sim 50\%$, and $\sim 45\%$ of the celestial sphere for J_2 values of 0, 0.005, and 0.05, respectively. Stability is defined as binaries with no disruptions after 10^5 years in the ensemble of numerical integrations (Section 3).

that an increasingly larger J_2 value results in an increase in the number of unstable orbit orientations in our simulations. These higher J_2 values cause collisions that can occur at a larger range of initial inclinations by increasing the maximum eccentricity acquired during a sequence of Kozai cycles. A larger maximum eccentricity therefore decreases the pericenter distance to allow for more frequent collisions (e.g., Nesvorný et al. 2003). We do not continue to observe this trend at high J_2 values greater than ~ 0.05 , where substantial primary oblateness prevents additional unstable orientations from forming.

4.3. Kozai-induced Disruptions End in Collisions

Here we discuss how disruptions due to the Kozai effect will result in collisions for typical NEA binaries. We only consider potential cases where the Kozai effect operates and can produce instabilities, and we assume these instabilities occur on much shorter timescales (on the order of tens to hundreds of years) compared to other perturbations such as planetary encounters, tidal evolution, and BYORP. We define disruptions as dynamical instabilities due to the Kozai effect, whose outcomes include (1) collisions between binary components and (2) ejections where the binary becomes unbound. The Kozai effect is capable of increasing a binary’s eccentricity, and very high eccentricities can cause the binary to become unbound or cause a collision between the binary components. An ejection occurs when an orbit’s apocenter Q , which is related to the semimajor axis a and the eccentricity e as $Q = a(1 + e)$, grows to a distance greater than the binary’s Hill radius R_{Hill} . A collision occurs when an orbit’s pericenter q , where $q = a(1 - e)$, is less than the primary radius R_p . R_{Hill} and R_p are known quantities given in Table 1. Therefore, for given R_{Hill} , R_p , and a , whether a gradually increasing eccentricity (i.e., due to the Kozai effect) causes a binary to undergo a collision or ejection is solely determined by the value of the eccentricity.

For all NEA binaries studied here (Table 1), values for their maximum Q (by assuming an e of 1) are much smaller than

their Hill radii. In order for Q to be as large as the Hill radius, if we assume a maximum e of 1 then any binary's semimajor axis needs to be at least half as large as the Hill radius in order for an ejection to occur. Thus, for any typical binary with a semimajor axis smaller than $0.5 R_{\text{Hill}}$, Kozai cycles will not cause ejections. On the other hand, collisions will occur at an eccentricity less than 1. Collisions will occur (by setting $q = R_p$) at the following e values for the binaries in our sample: 0.64 for 2002 CE26, 0.77 for 2004 DC, 0.94 for the hypothetical wide binary, 0.86 for 2003 YT1, 0.66 for Didymos, and 0.82 for 1991 VH. The specific case of the hypothetical wide binary is most interesting because we have already shown that the other binaries do not generally undergo Kozai cycles, let alone Kozai-induced instabilities. But for any wide NEA binary such as the hypothetical case examined here, if Kozai cycles are acting with sufficiently high inclinations to induce high eccentricities, collisions between binary components are the only possible instability outcome. The binary's pericenter will shrink below the primary radius before its apocenter can increase beyond the Hill radius and become unbound. Since collisions are the only instability outcome, this means that the Kozai effect cannot directly form asteroid pairs. It is possible that the Kozai effect may indirectly form asteroid pairs if a collision occurs but the components separate again and become unbound, or if the binary fortuitously makes a close planetary encounter during the short Kozai timescale.

For Kozai cycles in the absence of other perturbations, these collisions occur when the starting inclination results in a maximum eccentricity (Equation (1)) that is greater than the limiting eccentricities listed in the previous paragraph. Thus, for these starting inclinations, collisions will occur over the course of one Kozai cycle and repeated cycles will not occur. These disruption timescales are fast; for the hypothetical binary modeled after 1998 ST27, our longer-term (10^5 years) simulations show that from a starting eccentricity of 0.3, collisions occur ranging from ~ 3 years to $>10^4$ years later with the majority of collisions occurring within 100 years.

4.4. Formation of Contact Binaries

We discuss contact binary formation from large-amplitude Kozai oscillations. For wide binaries such as 1998 ST27 that can potentially undergo Kozai cycles even in the presence of primary oblateness, high starting inclinations can lead to high eccentricities (Equation (1)). During a single Kozai oscillation, these high eccentricities can drive the orbital pericenter distance to very low values and can cause the binary components to collide (see previous section for discussion on collisions). If a collision does not occur, tidal friction may play an important role and decrease the semimajor axis as well as the eccentricity. When the pericenter distance decreases due to high eccentricities, tides can more efficiently circularize the orbit by dissipating orbital energy during each pericenter passage (e.g., Perets & Naoz 2009; Fabrycky & Tremaine 2007). This leads to a circular orbit and a smaller semimajor axis.

If Kozai cycles and possibly tidal effects can cause binary components to come into contact with each other, this may be a mechanism to create near-Earth contact binaries, which constitute $\sim 10\%$ of NEAs larger than 200 m in diameter (Benner et al. 2006). If this process occurs, we would expect the observed contact binaries to have high obliquities preferentially between $\sim 40^\circ$ and $\sim 140^\circ$, assuming no significant obliquity evolution has occurred after formation of the contact binary. Obliquity is defined here as the inclination between the contact binary's

rotational angular momentum vector and the vector normal to its heliocentric orbital plane. This obliquity angle is equivalent to the inclination angle defined in Section 1 and used throughout the paper; we assume that the direction of an initially detached binary's orbital angular momentum vector is the same as the direction of a then-collided contact binary's rotational angular momentum vector.

Observed near-Earth contact binaries include Castalia (Hudson & Ostro 1994), Bacchus (Benner et al. 1999), Mithra (Brozovic et al. 2010), 1996 HW1 (Magri et al. 2011), and Itokawa (e.g., Ostro et al. 2004); all of which have high obliquities (M. W. Busch et al., in preparation). In the inner main belt, small binaries are observed with obliquities concentrated toward 0° and 180° and there is a lack of obliquities near 90° (Pravec et al. 2011). The concentration of binaries with low inclinations and the concentration of contact binaries near high inclinations hints that the Kozai effect may be effective at disrupting high-inclination binaries, but Pravec et al. (2011) have shown that the Kozai effect cannot completely explain the observed concentration of binaries with obliquities near 0° and 180° .

Although the Kozai effect is not responsible for the observed binary pole concentrations of small main belt binaries near 0° and 180° , it can be effective for more rarely observed NEA binaries with wide separations. Our simulations show that widely separated binaries can escape the dominating influence of primary oblateness to be significantly affected by solar perturbations. As a result, we suggest that wide binaries with eccentric or highly inclined orbits may become unstable under the effects of Kozai, leading to the formation of near-Earth contact binaries. Alternate theories of contact binary formation include low-velocity collisions between components in an unstable binary due to planetary encounters or radiative effects such as YORP and BYORP (e.g., Taylor & Margot 2011).

5. CONCLUSION

We explored the effect of Kozai cycles caused by the Sun on a sample of NEA binaries. Kozai oscillations can be suppressed by significant sources of pericenter precession; we identified three processes—primary oblateness (J_2), presence of an additional satellite, and tides—that contribute to orbital precession. We determined that primary oblateness is a dominant source of pericenter precession for small near-Earth satellites. Accordingly, we performed numerical simulations to evaluate the strength of Kozai cycles for NEA binaries in our sample with the inclusion of the primary's J_2 .

Our study showed that the binaries in our sample (with the exception of a hypothetical wide binary modeled after 1998 ST27) do not undergo Kozai cycles due to their small component separations. This sample includes all well-characterized binaries as defined by Fang & Margot (2012b) but does not include all observed binaries. Even the presence of a minimal J_2 (0.001) prevented NEA binaries in our sample from exhibiting signs of Kozai cycles. Consequently, we conclude that the Kozai effect is not relevant in explaining the observed characteristics of typical, observed NEA binaries. However, we note that the Kozai effect may have shaped the observed population of binaries by eliminating those binaries with very low- J_2 primaries or widely separated components.

For rarer observed cases of wide binaries, we studied a hypothetical wide binary modeled after 1998 ST27 whose large component separation indicated weaker J_2 effects and visible Kozai cycles at a wide range of possible J_2 values. For this

hypothetical wide binary, we were able to map out orbit pole orientations that are stable under Kozai effects. For cases of such wide binaries, the Kozai effect can lead to collisions between components. Accordingly, we suggest that the Kozai effect acting on widely separated binaries may be a route to the formation of near-Earth contact binaries.

We thank Simon Porter and the referee, Matija Ćuk, for useful discussions. This work was partially supported by NASA Planetary Astronomy Grant NNX09AQ68G.

REFERENCES

- Batygin, K., & Laughlin, G. 2011, *ApJ*, **730**, 95
- Benner, L. A. M., Hudson, R. S., Ostro, S. J., et al. 1999, *Icarus*, **139**, 309
- Benner, L. A. M., Margot, J. L., Nolan, M. C., et al. 2010, *BAAS*, **42**, 1056
- Benner, L. A. M., Nolan, M. C., Ostro, S. J., et al. 2006, *Icarus*, **182**, 474
- Blaes, O., Lee, M. H., & Socrates, A. 2002, *ApJ*, **578**, 775
- Botke, W. F., Morbidelli, A., Jedicke, R., et al. 2002, *Icarus*, **156**, 399
- Brozovic, M., Benner, L. A., Taylor, P. A., et al. 2011, *Icarus*, **216**, 241
- Brozovic, M., Benner, L. A. M., Magri, C., et al. 2010, *Icarus*, **208**, 207
- Chambers, J. E. 1999, *MNRAS*, **304**, 793
- Ćuk, M. 2007, *ApJ*, **659**, L57
- Ćuk, M., & Burns, J. A. 2005, *Icarus*, **176**, 418
- Ćuk, M., & Nesvorný, D. 2010, *Icarus*, **207**, 732
- Eggleton, P. P., & Kiseleva-Eggleton, L. 2001, *ApJ*, **562**, 1012
- Eggleton, P. P., & Kiseleva-Eggleton, L. 2006, *Ap&SS*, **304**, 75
- Fabrycky, D., & Tremaine, S. 2007, *ApJ*, **669**, 1298
- Fang, J., Margot, J., Brozovic, M., et al. 2011, *AJ*, **141**, 154
- Fang, J., & Margot, J.-L. 2012a, *AJ*, **143**, 25
- Fang, J., & Margot, J.-L. 2012b, *AJ*, **143**, 24
- Goldreich, P. 1963, *MNRAS*, **126**, 257
- Goldreich, P., & Sari, R. 2009, *ApJ*, **691**, 54
- Harrington, R. S. 1968, *AJ*, **73**, 190
- Holman, M., Touma, J., & Tremaine, S. 1997, *Nature*, **386**, 254
- Hudson, R. S., & Ostro, S. J. 1994, *Science*, **263**, 940
- Innanen, K. A., Zheng, J. Q., Mikkola, S., & Valtonen, M. J. 1997, *AJ*, **113**, 1915
- Jacobson, S. A., & Scheeres, D. J. 2011, *ApJ*, **736**, L19
- Katz, B., & Dong, S. 2011, arXiv:1105.3953
- Kiseleva, L. G., Eggleton, P. P., & Mikkola, S. 1998, *MNRAS*, **300**, 292
- Kozai, Y. 1962, *AJ*, **67**, 591
- Lithwick, Y., & Naoz, S. 2011, *ApJ*, **742**, 94
- Magri, C., Howell, E. S., Nolan, M. C., et al. 2011, *Icarus*, **214**, 210
- Mardling, R. A. 2007, *MNRAS*, **382**, 1768
- Margot, J., Taylor, P. A., Nolan, M. C., et al. 2008, *BAAS*, **40**, 433
- Margot, J. L., Nolan, M. C., Benner, L. A. M., et al. 2002, *Science*, **296**, 1445
- Mazeh, T., Krymowski, Y., & Rosenfeld, G. 1997, *ApJ*, **477**, L103
- Mazeh, T., & Shaham, J. 1979, *A&A*, **77**, 145
- McMahon, J., & Scheeres, D. 2010a, *Icarus*, **209**, 494
- McMahon, J., & Scheeres, D. 2010b, *Celest. Mech. Dyn. Astron.*, **106**, 261
- Murray, C. D., & Dermott, S. F. (ed.) 1999, *Solar System Dynamics* (Cambridge: Cambridge University Press)
- Naoz, S., Farr, W. M., Lithwick, Y., Rasio, F. A., & Teyssandier, J. 2011, *Nature*, **473**, 187
- Nesvorný, D., Alvarellos, J. L. A., Dones, L., & Levison, H. F. 2003, *AJ*, **126**, 398
- Nicholson, P. D., Ćuk, M., Sheppard, S. S., Nesvorný, D., & Johnson, T. V. 2008, in *Irregular Satellites of the Giant Planets*, ed. M. A. Barucci, H. Boehnhardt, D. P. Cruikshank, A. Morbidelli, & R. Dotson (Tucson, AZ: Univ. Arizona Press), 411
- Nolan, M. C., Howell, E. S., & Miranda, G. 2004, *BAAS*, **36**, 1132
- Ostro, S. J., Benner, L. A. M., Nolan, M. C., et al. 2004, *Meteorit. Planet. Sci.*, **39**, 407
- Ostro, S. J., Margot, J.-L., Benner, L. A. M., et al. 2006, *Science*, **314**, 1276
- Perets, H. B., & Naoz, S. 2009, *ApJ*, **699**, L17
- Pravec, P., Scheirich, P., Kušnirák, P., et al. 2006, *Icarus*, **181**, 63
- Pravec, P., Scheirich, P., Vokrouhlický, D., et al. 2011, in *EPSC-DPS Joint Meeting 2011*, **312**, <http://meetings.copernicus.org/epsc-dps2011>
- Ragozzine, D., & Brown, M. E. 2009, *AJ*, **137**, 4766
- Shepard, M. K., Margot, J.-L., Magri, C., et al. 2006, *Icarus*, **184**, 198
- Steinberg, E., & Sari, R. 2011, *AJ*, **141**, 55
- Sterne, T. E. 1939, *MNRAS*, **99**, 451
- Takeda, G., & Rasio, F. A. 2005, *ApJ*, **627**, 1001
- Taylor, P. A., & Margot, J. L. 2011, *Icarus*, **212**, 661
- Taylor, P. A., Margot, J. L., Nolan, M. C., et al. 2008, in *Asteroids, Comets, Meteors* (LPI Contributions, No. 1405; Baltimore, MD: LPI), **8322**
- Thomas, F., & Morbidelli, A. 1996, *Celest. Mech. Dyn. Astron.*, **64**, 209
- Tremaine, S., & Zakamska, N. L. 2004, in *AIP Conf. Ser. 713, The Search for Other Worlds*, ed. S. S. Holt & D. Deming (Melville, NY: AIP), **243**
- Vallado, D. A. (ed.) 2001, *Fundamentals of Astrodynamics and Applications* (El Segundo, CA: Microcosm Press)
- Walsh, K. J., Richardson, D. C., & Michel, P. 2008, *Nature*, **454**, 188